Damage mechanics based modelling of the relation between capillary pores and compressive strength of concrete

S. Akyuz, Y. Akkaya, H.O. Yazan & M.A. Tasdemir
Istanbul Technical University, Civil Engineering Faculty, Istanbul, Turkey

ABSTRACT: The amount and geometry of pores in hardened cement paste phase, that affect the mechanical behaviour of concrete, have been considered in the form of two different parameters: porosity and capillary sorptivity coefficient (or water/cement ratio) where the latter represents the geometry of pores in hardened concrete. A mathematical model based on the damage mechanics approach has been developed to relate the compressive strength of concrete to these two parameters. Equations developed in this model have been applied to the values obtained in an available experimental work, in which porosities, sorptivity coefficients and strengths were measured for 40 different concrete mixtures. For indirect determination of the water-cement ratio in both hardening and hardened concretes, a petrographic examination method using optical fluorescence is presented. Additionally, five concrete mixtures with different water-cement ratios were used to determine their fluorescence intensities, sorptivity coefficients and compressive strengths. It is shown that the flouresscence intensity is directly affected by the water-cement ratio of concrete. Good agreement has been found between experimental and calculated results.

1 INTRODUCTION

Concrete is an extremely complex system of solid phases, pores, and water, with a high degree of heterogeneity. It has been shown that the pore size distribution in the cement paste in concrete and in mortar is different from that of plain cement paste, which does not contain aggregate (Winslow & Cohen 1994). Additional large pores occur at the interfacial zones surrounding each aggregate. The interface between cement paste and coarse aggregate particles is the weakest zone, and the use of particles, such as silica fume, is important for densification and for the improvement of the stability of fresh concrete, thus enhancing overall durability and strength. For material modeling purpose, concrete can be considered as a three-phase composite material consisting of hardened cement paste, aggregate, and the interfacial zone between aggregate and cement paste (Tasdemir et al. 1998). To gain benefits from the inclusions of fine particles, good dispersion within the concrete system is necessary and is provided by means of high range water reducing admixtures (Sawicz & Heng 1996, Detwiller & Mehta 1989, Nehdi et al. 1996). Recent studies have shown that measurements of permeability of concrete can be used as an indication of durability. Dinku & Reinhardt (1997) have shown that the gas permeability is sensitive to changes in curing duration, water/cement ratio, age of testing and moisture history of concrete; according to their research, it is possible to predict the gas permeability from the capillary sorptivity measurements. According to Martys & Ferraris (1997), the sorptivity coefficient is essential to predict the service life of concrete as a structural material and to improve its performance. Since the pore structure has a dominant factor on the performance of concrete, the main objective of this work is to develop a combined approach for quality control of concrete using optical fluorescence microscopy, sorptivity measurements, and damage mechanics based modeling. It is thought that this approach will help to fill the need in bringing the theoretical concepts to implementation for the better understanding of the material behaviour.

2 THEORETICAL BACKGROUND

The close neighbourhood of a crack can be accepted as not being able to carry the load, i.e. in this region the stress is zero. v_0 is the volume which is able to carry load and υ is the total volume of the solid body. υ-v_0 and υ-v=H show the dead volume of the solid body under unloaded and loaded conditions, respectively. v is the total volume of the solid body under load. There is a well known relation of

geometry between the area of crack surface A and the total dead volume H given as

$$A^{3/2} = kH = k(\upsilon - v) \tag{1}$$

where k is a constant (Akyuz et al. 2000). When $v=v_0$, A is A_0, hence A/A_0 can be expressed as

$$\frac{A}{A_0} = \left(\frac{\upsilon - v}{\upsilon - v_0}\right)^{2/3} \tag{2}$$

Here A_0 is the area of crack surface in the solid when U=V=0 (U is the work done by the external loads, V is the elastic component of the stored energy, Akyuz et al. 2000). Let us consider the stress-strain curve of concrete under uniaxial compressive loading and if the total volume of the concrete specimen is υ, the work done by the external forces can be written as

$$U = \left\{\int_0^{\varepsilon} \sigma(\varepsilon)\, d\varepsilon\right\}\upsilon \tag{3}$$

where σ and ε are uniaxial stress and strain, respectively. The reversible (elastic) work is

$$V = \frac{1}{2}\cdot\frac{\sigma^2}{E_{ef}}\cdot\upsilon \tag{4}$$

where E_{ef} is the effective modulus of elasticity which is slightly less than the dynamic modulus of elasticity, E_d. For the simplicity in calculations, it is assumed that $E_{ef} \approx E_d$. From Equations 3 and 4, the following equation can be written (Akyuz et al. 2000)

$$\int_0^{\varepsilon} \sigma(\varepsilon)\, d\varepsilon - \frac{1}{2}\cdot\frac{\sigma^2}{E_d} = \gamma_F \cdot \frac{A_0}{\upsilon}\cdot\left(\frac{A}{A_0} - 1\right) \tag{5}$$

where γ_F is the amount of energy required to create a unit area of fracture surface. If we take the differential of both sides, then we have

$$\sigma - \alpha\sigma\dot{\sigma} = \beta\frac{d}{d\varepsilon}\left(\frac{a}{a_0} - 1\right) \tag{6}$$

where $a=A/\upsilon$, $a_0=A_0/\upsilon$, $\beta=a_0\gamma_F$ and $\alpha=1/E$. The damage function can be defined as

$$\psi = \frac{v}{v_0} = \begin{cases} 1\,, & \varepsilon = 0 \\ \dfrac{v}{v_0}, & 0 < \varepsilon < \varepsilon_m \\ 0\,, & \varepsilon = \varepsilon_m \end{cases} \tag{7}$$

ε_m is defined as the strain at compressive strength. As shown from Equation 7, ψ is a decreasing function and as result $\dot{\psi}<0$. From Equation 2 a/a_0 can be written as

$$\frac{a}{a_0} = \left(\frac{\dfrac{\upsilon}{v_0} - \dfrac{v}{v_0}}{\dfrac{\upsilon}{v_0} - 1}\right)^{2/3} = \left(\frac{q - \dfrac{v}{v_0}}{q-1}\right)^{2/3} \tag{8}$$

where $q=\upsilon/v_0>1$ which is a constant. In this case, the following equation can be expressed as

$$\frac{d}{d\varepsilon}\left(\frac{a}{a_0} - 1\right) = -\frac{2}{3}\cdot\frac{1}{(q-1)^{2/3}(q-\psi)^{1/3}}\cdot\frac{d\psi}{d\varepsilon} \tag{9}$$

Substitution of Equation 9 into Equation 6, the kinetic equation of damage can be obtained as

$$\dot{\psi} = \frac{d\psi}{d\varepsilon} = -K(q-\psi)^{1/3}(\sigma - \alpha\sigma\dot{\sigma}) \tag{10}$$

where $K=(3/2)(q-1)^{2/3}/\beta$. In a quasi-static case, the damage does not increase under a constant stress σ_0 for $\sigma_0 < f_c$, where f_c is the compressive strength of concrete. It is assumed that, the failure occurs near the peak point under a constant stress $\sigma_0 \approx f_c$. In this case, the differential equation becomes

$$\frac{d\psi}{(q-\psi)^{1/3}} = -Kf_c\cdot d\varepsilon \tag{11}$$

Taking the integration of Equation 11 with $\psi=1$ at $\varepsilon=0$ and $\psi=0$ at $\varepsilon=\varepsilon_m$, then f_c can be written as

$$f_c = \gamma_F\frac{a_0}{\varepsilon_m}\left[\frac{1}{\left(1 - \dfrac{1}{q}\right)^{2/3}} - 1\right] \tag{12}$$

On the other hand, if we take a_m as the maximum area of crack surface per unit volume, then $a_0/a_m=(1-1/q)^{2/3}$. It is known that when ε_m increases, the area of crack surface also increases. From this point of view, we assume that $\varepsilon_m=a_m\eta$, thus we have

$$f_c = \frac{\gamma_F}{\eta}\left[1 - \left(1 - \frac{1}{q}\right)^{2/3}\right] \tag{13}$$

We assume that G is the volume of concrete excluding the crack. Hence, we can write the inequality of $v_0/\upsilon \le G/\upsilon \le 1$. On the other hand, as shown in Fig-

ure 1, when $G/\upsilon=0$, then $v_0/\upsilon=0$ and when $G/\upsilon=1$, then $v_0/\upsilon=1$. Thus, v_0/υ can be written as

$$\frac{v_0}{\upsilon}=\left(\frac{G}{\upsilon}\right)^m, m\geq 1 \quad (14)$$

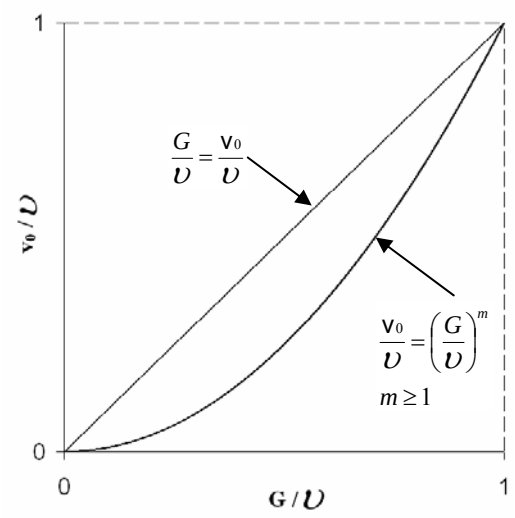

Figure 1. v_o/υ versus G/υ

Substituting of v_0/υ given in Equation 14 into Equation 13, the following equation can be obtained:

$$f_c=M\left\{1-\left[1-(1-p)^m\right]^{2/3}\right\} \quad (15)$$

where $M=\gamma_F/\eta$ and $m=1+\theta C$, in which C is the capillary coefficient or $m=1+\theta(w/c-0.23)$, in which w/c is the water/cement ratio. In Equation 15, M is the highest compressive strength of the material which corresponds to the zero porosity. As shown in Figure 1, m is a parameter which represents pore geometry. In case of spherical pore, there is no region without stress around the pore, thus $k=G/\upsilon=v_0/\upsilon$ and m=1. As the sphere type of pore turns into an elliptical shape, m takes the values greater than one and the stress concentration increases, as a result compressive strength of concrete decreases. Thus, pore geometry can be determined by means of capillary pores as given above. According to the proposed model depending on the equation chosen from m, the compressive strength of concrete (f_c) can be written as

$$f_c=M_1\left\{1-\left[1-(1-p)^{1+\theta_1 C}\right]^{2/3}\right\} \quad (16)$$

or

$$f_c=M_2\left\{1-\left[1-(1-p)^{1+\theta_2\left(\frac{w}{c}-0.23\right)}\right]^{2/3}\right\} \quad (17)$$

where M_1 and M_2 are constants which represent the theoretical compressive strength of concrete without porosity (maximum strength), p is the porosity, C is the capillary coefficient as in Equation 16 and w/c is the water/cement ratio as in Equation 17 and θ_1 and θ_2 are the constants of these equations.

3 EXPERIMENTS

3.1 *Materials*

The test results used in this work were obtained at the Istanbul Technical University (ITU). The combined study of experiments, the damage mechanics based approach explained above, prediction of the water-cement ratio using the optical fluorescence microscopy, capillary sorptivity and compressive strength of concrete are elaborated.

Locally available sea sand of the Istanbul area, a Portland cement (CEM I-42,5), crushed limestone and its fines were used in the mixtures. The grading and maximum aggregate size of concrete were kept constant. Mix proportions of sand, limestone fines and crushed limestone were 35%, 15%, and 50% respectively. Five concrete batches were made with the same Portland cement, sand and limestone, and its fines.

At least three specimens of each concrete mixture were tested at 126 days.

3.2 *Sorptivity tests*

Three test specimens for sorptivity test, cut from the cylinders of 100 mm diameter, were prepared for each mixture. Measurement of capillary sorption were carried out using specimens pre-conditioned in the oven at about 50°C until constant mass.

Test specimens were exposed to the water on the surface of 7854 mm^2 by placing in a pan. The water level in the pan was maintained at about 5mm above the base of the specimens during this experiment. The lower areas on the sides of the specimens were coated with epoxy to achieve unidirectional flow. At certain times, the masses of the specimens were measured using a balance, then the amount of water absorbed was calculated and normalized with respect to the cross-section area of the specimens exposed to the water at various times such as 1, 2, 3, 5, 10, 20, 30, 60, 120, 180, 240, 300 and 360 minutes (Figure 2).

The sorptivity coefficient (k), was obtained by using the following expression:

$$\left(\frac{Q}{A}\right)^2=k\cdot t \quad (18)$$

where Q = the amount of water absorbed [cm^3]; A = the cross-sectional area of specimen that was in contact with water [cm^2]; k = the sorptivity coefficient of the specimen [cm^2/min]; t = time [min].

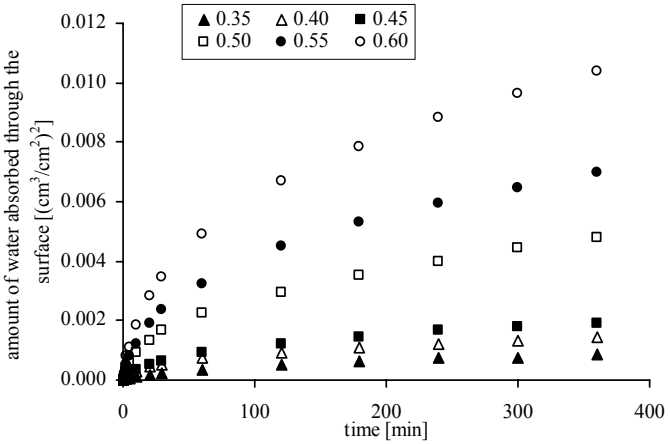

Figure 2. Time versus amount of water absorbed through the surface

To determine the sorptivity coefficient, $(Q/A)^2$ was plotted against the time (t), then, k was calculated from the slope of the linear relation between $(Q/A)^2$ and t.

As seen in Figure 3, 4 and 5 the sorptivity coefficient of concrete decreases with increasing compressive strength of concrete. Similar trend was obtained by Tasdemir (2003), as test results indicate that the sorptivity coefficient of concrete decreases as the compressive strength of concrete increases. It was also shown that the sorptivity coefficient of concrete is very sensitive to the curing condition and the sorptivity coefficient of concrete is higher in low strength concrete.

Thus, concrete has larger capillary pores and lower compressive strength when a higher capillary sorption in concrete is obtained. In Figures 3, 4 and 5, the parameters M_i and θ_i can be calculated using the data obtained. Figures 6 and 7 show the relation between w/c ratio and compressive strength of concrete.

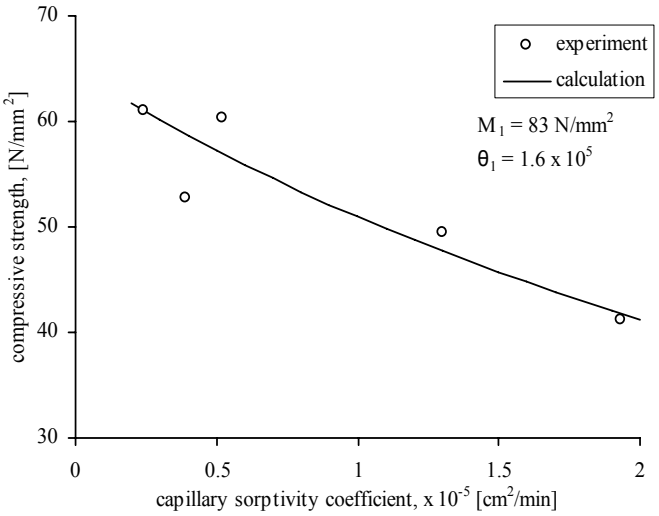

Figure 3. Sorptivity coefficient versus compressive strengths of concrete (p=0.10)

Equations developed by Akyuz et al. (2000) above were tested using the experimental data obtained from 40 different concrete mixtures. In each mixture the total porosity, the capillary coefficient and the compressive strength of concrete were measured (Uyan 1974).

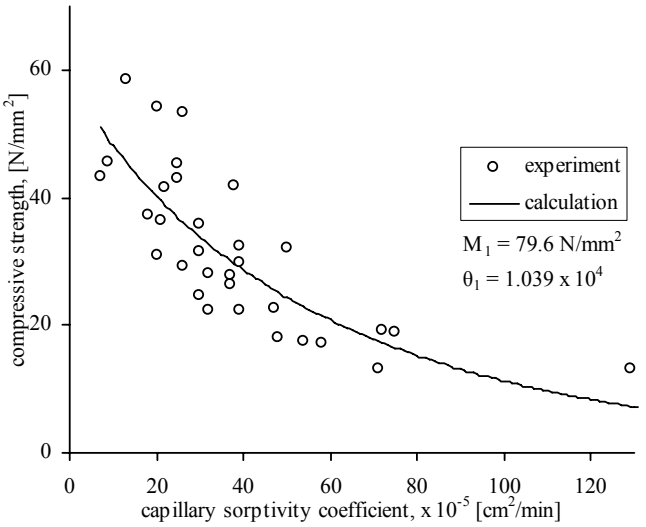

Figure 4. Capillary sorptivity coefficient versus compressive strength of concrete (p=0.13), experiments from Uyan (1974)

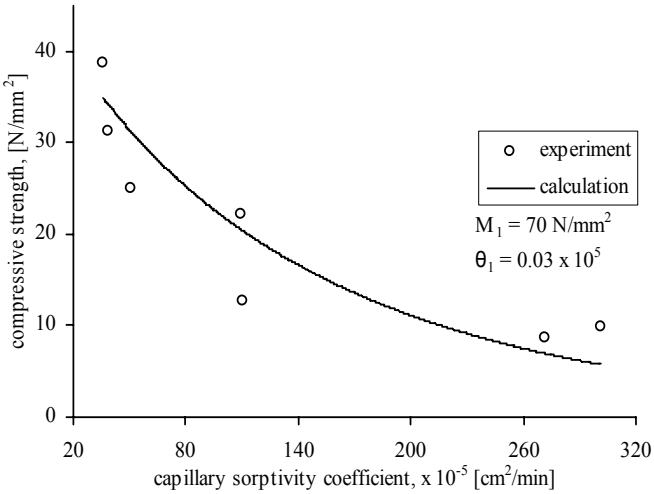

Figure 5. Capillary sorptivity coefficient versus compressive strength of concrete (p=0.19) , experiments from Uyan (1974)

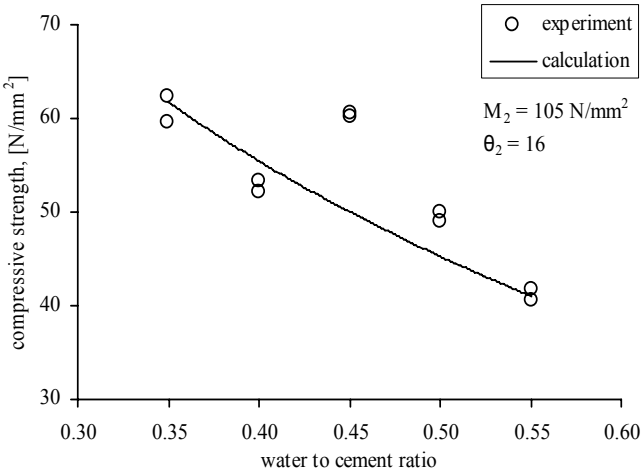

Figure 6. Variation of compressive strength with w/c ratio (p=0.10)

In the first 31 different mixtures, porosity was in between 0.11 and 0.15, with an average value of 0.13. For the rest of the mixtures, the porosity values was between 0.17 and 0.21 and the average was 0.19.

The parameters M_i and θ_i were calculated using the data given by Uyan (1974). The curves obtained by substituting these parameters in Equation 16 and 17 were given in Figures 4, 5 and 7 together with the parameters. Good agreement obtained between the experimental and theoretical results shows that the amount of porosity as well

as the geometry of pores can be related to the compressive strength of concrete.

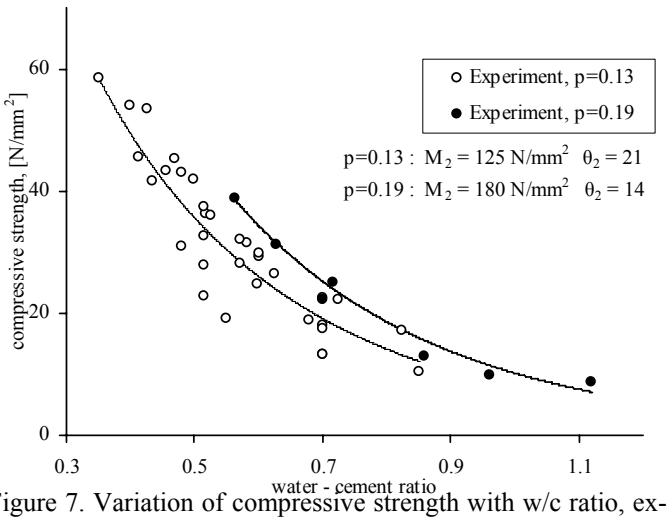

Figure 7. Variation of compressive strength with w/c ratio, experiments from Uyan (1974)

3.3 *Determination of w/c ratio using optical fluorescence microscopy*

In hardened concrete, it is not possible to determine the water-cement ratio directly. However, there is an indirect method for determining the water-cement ratio in hardening concrete for both quality control at the early ages and the forensic investigation of deteriorated concrete (Jacobsen et al. 2000).

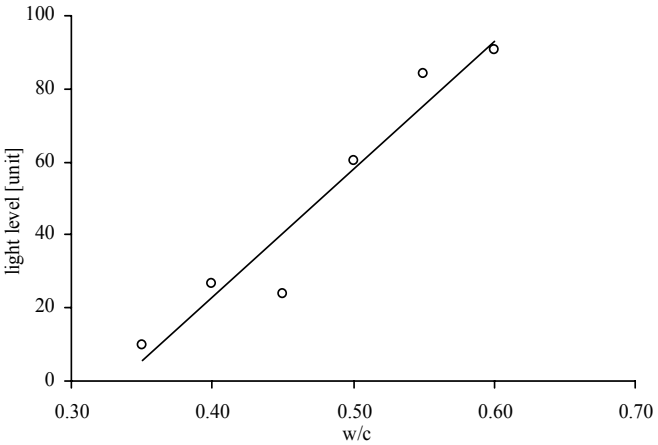

Figure 8. Relation between light level in the thin section and w/c ratio of concrete

Modern concrete contains a variety of organic admixtures, supplementary cementitious materials, manufactured aggregates, special cements, and various types of fibers. These materials are added to the mixture to improve the properties of the concrete, enhance its performance, or control specific properties such as setting time, heat of hydration, shrinkage and workability (Powers 2006). In recent years, optical fluorescence microscopy of concrete has been used as a tool to investigate the internal structure of hardened concrete. Several attempts have been made to determine the water-cement ratio in concrete using optical fluorescent microscopy (Jacobsen et al. 2000; Henrichsen & Laugesen 1995, Laugesen 1993, Mayfield 1990).

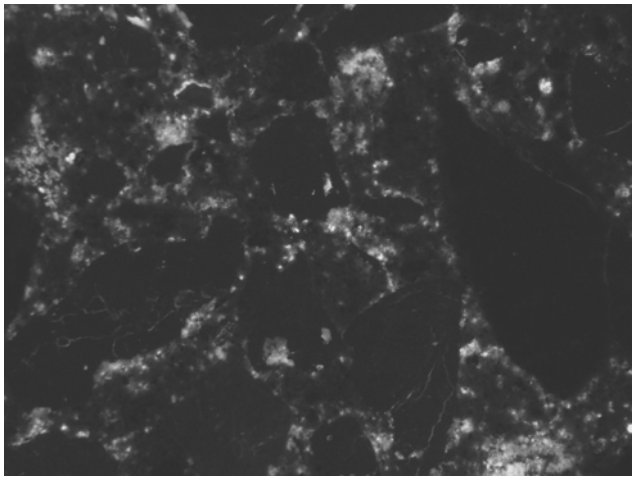

w/c=0.40

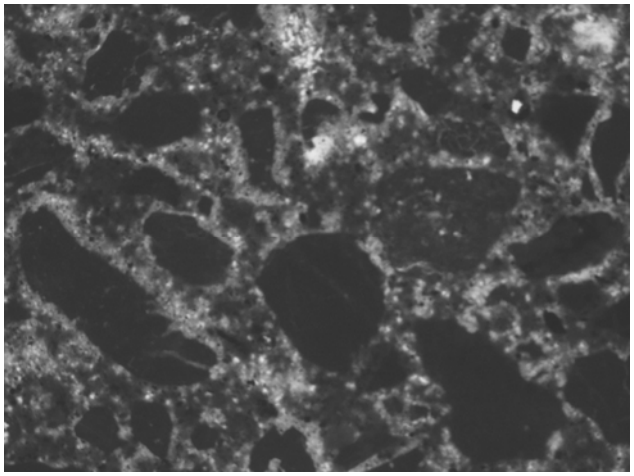

w/c=0.50

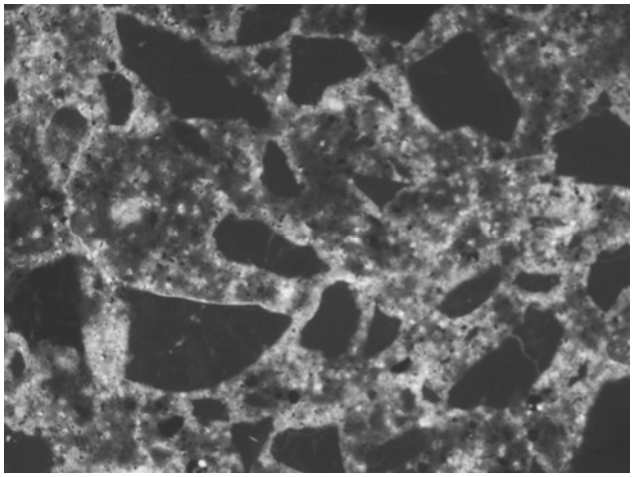

w/c=0.60

Figure 9. Photographs of samples taken under the fluorescent light with water-cement ratios of 0.40, 0.50, and 0.60

The method used in concrete petrography has been borrowed from geology and it is based on vacuum impregnation of concrete using a yellow fluorescent epoxy. During impregnation the capillary porosity, cracks, voids, and defects in the concrete are filled with epoxy. After impregnation, thin sections are prepared from slices of concrete that are attached to a glass slide, and then ground to a thickness of about 20μm to 30μm. These thin sections allow the concrete petrographer to identify the material constituents and predict their proportions , air content, water-cement ratio, paste homogeneity, paste volume, aggregate volume, effectiveness of curing, and examine the relationships between the various constituents.

The impregnation depth of the fluorescent epoxy into the sample is dependent on the capillary porosity of the cement paste (Laugesen 1993). Large cracks, cement paste-aggregate debonding, interconnected porosity, and air voids can be easily impregnated.

In Figure 8, as the water-cement ratio of concrete increases, the fluorescence intensity increases significantly. After obtaining such a calibration curve in laboratory conditions, water-cement ratio of concrete in-situ can be indirectly predicted providing sufficient measurement.

In Figure 9, as the water-cement ratio of concrete increases from 0.40 to 0.60, the lightness increases substantially. Hence, the increase in the capillary porosity at the higher water-cement ratios results in high flourescence intensity. However, at the lower water-cement ratios, the thin section becomes darker.

4 CONCLUSIONS

The dependence of compressive strength on the capillary coefficient or water-cement ratio is succesfully represented by the proposed model, based on damage mechanics. The model described here not only depends on the effect of pore volume, but also on the geometry of pores on the compressive strength of concrete.

In petrographic examination of concrete air-void system parameters, paste content and crack widths can be measured. The water-cement or water-binder ratio, air content, extent of cement hydration, paste and aggregate volumes can be predicted. Especially, after obtaining the relationship between the light level in the thin section and the water-cement ratio in the laboratory condition, the quality control of concrete in-situ can be realized using an optical fluorescence microscopy.

ACKNOWLEDGMENTS

This research was carried out in the Faculty of Civil Engineering at Istanbul Technical University (ITU). The authors wish to acknowledge the financial support of TUBITAK (The Scientific & Technological Research Council of Turkey): Project:106G122, 1007-Kamu.

REFERENCES

Akyuz,S., Tasdemir,M.A. & Uyan,M. 2000. Pore effects on the compressive strength of concrete, *Concrete 2000*, Editors: Dhir,R.K. and Jones M.R., E&FN SPON: 1407-1416.

Detwiller,R.J. & Mehta,P.K. 1989. Chemical and physical effects of silica fume on mechanical behavior of concrete, *ACI Materials Journal*, 86: 609-614.

Dinku,A. & Reinhardt,H.W. 1997. Gas permeability coefficient of cover concrete as a performance control, *Materials and Structures*, 30: 387-393.

Henrichsen,A. & Laugesen,P. 1995. "Monitoring of Concrete Quality in High Performance Civil Engineering Constructions," *MRS Symposium Proceedings* 370: 49-56.

Jakobsen UH, Laugesen P. & Thaulow N. 2000. Determination of water to cement ratio in hardened concrete by optical fluorescence microscopy. *ACI SP-191, Water–cement ratio and other durability parameters—techniques for determination*: 27–42.

Laugesen,P. 1993. Effective w/c ratio of cement paste in concrete. *Proc. 4th Euroseminar on Microscopy Applied to Building Materials, Wisby, Sweden.*

Martys,N.S. & Ferraris,C.F. 1997. Capillary transport in mortars and concrete, *Cement and Concrete Research*, 27: 747-760.

Mayfield,B. 1990. The quantitative evaluation of the water/cement ratio using flourescence microscopy. *Magazine of Concrete Research*, 150: 45-49.

Nehdi,M., Mindess,S. & Aïtcin,P.C. 1996. Optimization of high strength limestone filler cement mortars, *Cement and Concrete Research*, 26: 883-893.

Powers,L.J. 2006. The power of petrography, *Structure Magazine*, January: 25-28.

Sawicz,Z. & Heng,S.S. 1996. Durability of concrete with addition of limestone powder, *Magazine of Concrete Research*, 48: 131-137.

Tasdemir,M.A., Tasdemir, C., Akyuz, S., Jefferson, A.D., Lydon,F.D., & Barr, B.I.G. 1998. “Evaluation of Strains at Peak Stresses in Concrete: A Three Phase Composite Model Approach”, *Cement and Concrete Composites*, 20: 301-318.

Tasdemir,C. 2003. Combined effects of mineral admixtures and curing conditions on the sorptivity coefficient of concrete, *Cement and Concrete Research*, 33: 1637-1642.

Uyan,M. 1974. Capillary in concrete. PhD thesis, Faculty of Civil Engineering, Istanbul Technical University: 180p (in Turkish with English summary).

Winslow, D.N. & Cohen, M.D. 1994. Percolation and pore structure in mortars and concrete, *Cement and Concrete Research*, 24: 25-37.